Postprint of: Koziel S.; Pietrenko-Dabrowska A, Reduced-cost electromagnetic-driven optimisation of antenna structures by means of trust-region gradient-search with sparse Jacobian updates, IET Microwaves, Antennas & Propagation, 2019, 13, (10), p. 1646-1652, DOI: 10.1049/iet-map.2018.5879

Reduced-Cost EM-driven Optimization of Antenna Structures By Means of Trust-Region Gradient-Search with Sparse Jacobian Updates

Slawomir Koziel[1,2] and Anna Pietrenko-Dabrowska[2]

[1] Engineering Optimization & Modeling Center, School of Science and Engineering, Reykjavik University, Menntavegur 1, 101 Reykjavik, Iceland
koziel@ru.is

[2] Faculty of Electronics, Telecommunications and Informatics, Gdansk University of Technology, Narutowicza 11/12, 80-233 Gdansk Poland
anndabr1@pg.edu.pl

Abstract: Numerical optimization plays more and more important role in the design of antennas and antenna systems. In particular, because of lack of design-ready theoretical models, electromagnetic (EM)-simulation-driven adjustment of geometry parameters is a necessary step of the design process. At the same time, parameter sweeping traditionally used for that purpose cannot handle complex topologies and a large number of variables utilized for antenna parameterization. On the other hand, a problem pertinent to conventional optimization routines is their high computational cost, which can be reduced using, e.g., surrogate-assisted techniques. Still, direct optimization of EM simulation antenna models is required at certain level of fidelity. This work proposes a reduced cost trust-region algorithm with sparse updates of the antenna response Jacobian, which are decided based on relocation of the design variable vector between algorithm iterations as well as the update history. Our approach permits significant reduction of the number of EM analyses during the optimization run without affecting the quality of the final design in a significant manner. Robustness of the proposed technique is validated using a set of benchmark antenna structures, statistical analysis of the algorithm performance over multiple initial designs, as well as investigating the effects of its control parameters, some of which permit control of efficiency vs. design quality trade-off. Selected designs were fabricated and measured to validate the computational models utilized in the optimization process. Typical computational savings are around 40 percent as compared to the reference algorithm.

1. Introduction

Design of contemporary antenna systems heavily exploits electromagnetic (EM) simulation tools. Complex antenna topologies lack reliable theoretical models and EM-driven design closure is a necessary step to improve the performance figures pertinent to electrical and field characteristics of the structure at hand (e.g., impedance matching, gain, size, or axial ratio). This is realized by adjustment of geometry and/or material parameters [1]. Perhaps the most common design closure approach is still parameter sweeping guided by engineering experience. Practical applicability of this method is limited to relatively simple designs. Proper handling of complex antenna geometries described by a large number of parameters requires formal optimization. Unfortunately, conventional algorithms, including both local [2], [3], and global methods (the latter mostly involving population-based metaheuristics [4]-[6]) are computationally expensive, often to the extent of being prohibitive. This high cost originates from a large number of full-wave electromagnetic (EM) analyses required by the algorithms to converge. At the same time, EM simulation is required to ensure sufficient level of accuracy of antenna evaluation.

Clearly, a key prerequisite for solving the high cost issue is the reduction of the number of expensive EM simulations required by the optimization procedures. Several classes of techniques have been developed and applied over the years, including, among others, adjoint sentivities [7], [8] and a variety of surrogate-assisted methods (e.g. [1]). Until now, adjoints have been only supported by only a few commercial EM simulation packages (e.g., [9]). Surrogate-assisted techniques are founded on the concept of a fast replacement model (also referred to as surrogate). The surrogate is constructed either from sampled high-fidelity EM model data (data-driven models) or an underlying low-fidelity model (physics-based surrogates), then iteratively refined and re-optimized to yield approximations to the optimum design at low computational cost [10]. One of the most popular physics-based surrogate-assisted methods in microwave and antenna engineering is space mapping (SM) [11], other techniques include various response correction algorithms [12], [13], feature-based optimization [14], adaptive response scaling [15], as well as combination of deterministic algorithms with machine learning procedures (e.g., [16]). The fact that physics-based surrogates so heavily rely on low-fidelity models is a limiting factor from the point of view of antenna applications. This is because the low-fidelity antenna models are normally obtained through course-mesh EM simulations (thus, they are relatively expensive). Data-driven surrogates are more generic with practical methods involving kriging interpolation [17] or Gaussian Process Regression (GPR) [18]. However, reliable data-driven antenna surrogates can only be constructed in low-dimensional parameter spaces. Another application is construction of local surrogates, for example, for the purpose of uncertainty quantification [19].

In this paper, a novel gradient-based optimization technique with numerical derivatives for reduced-cost optimization of antenna structures is presented. It is a modification of a conventional trust-region (TR) framework, where the antenna response sensitivities (represented by a Jacobian matrix) are not updated upon each successful iteration, but in a sparse manner which is controlled by relative relocation (with respect to the current search region) of the design between algorithm iterations. The history of Jacobian updates as well as the absolute search region size are also taken into account. The updates are put off for variables exhibiting limited design relocation, which results in lowering the overall optimization cost.

For the sake of validation, the proposed methodology has been tested on a set of benchmark wideband antennas from the literature. Optimization runs have been performed for a number of random initial designs in order to obtain statistical data necessary to assess the algorithm robustness. The results indicate consistent behaviour with considerable saving of around 40 percent on average as compared to the reference algorithm. Additional experiments also indicate a possibility of trading-off the computational savings for improved design quality. The algorithm described in the paper can be utilized to speed up direct optimization of antenna structure, but also to accelerate physics-based surrogate-assisted procedures, specifically, solving sub-problems that require multiple evaluations of coarse-discretization models (e.g., within multi-fidelity design frameworks, both single- [1] and multi-objective ones [10]).

2. Reduced-Cost Antenna Optimization by Sparse Jacobian Updates

Here, a formulation of EM-driven design closure of antenna structures is recalled along with the outline of the conventional trust-region gradient-search algorithm. Subsequently, the proposed approach is discussed, the key of which is a Jacobian update management scheme.

2.1. Antenna Design Closure as Optimization Task

The response (e.g., reflection or gain characteristics versus frequency, etc.) of a full-wave EM-simulation antenna model will be denoted as $\boldsymbol{R}(\boldsymbol{x})$. Design closure is understood here as an adjustment of geometry parameter values assuming fixed antenna topology. The antenna dimensions are represented by the vector $\boldsymbol{x}$. The optimum design is sought as a solution to the following nonlinear minimization problem

$$\boldsymbol{x}^* = \arg\min_{\boldsymbol{x}} U(\boldsymbol{R}(\boldsymbol{x})) \tag{1}$$

In (1), U stands for the objective function. In general, the analytical form of U depends on what particular figures of interest are considered and what are the design constraints. As this work focuses on the algorithmic aspect of the optimization process, without loss of generality, we consider a specific problem of improving in-band reflection of the antenna structure at hand, or, minimization of the maximum in-band reflection $|S_{11}(\boldsymbol{x},f)|$. In this case, the function U takes the form

$$U(\boldsymbol{R}(\boldsymbol{x})) = \max_{f\in F} |S_{11}(\boldsymbol{x},f)| \tag{2}$$

where F is the frequency range of interest (e.g., 3.1 GHz to 10.6 GHz in case of UWB antennas). The problem (1), (2) is formulated in a minimax sense. This type of formulation is one of the most popular ones. Other, often used formulations include maximization of the antenna bandwidth (at −10 dB level), maximization of gain, reducing sidelobe level (for array antennas), or explicit reduction of the antenna footprint. Particular acceptance thresholds of selected figures of interest can also be used as design constraints [20], [21].

2.2. Reference Algorithm: Trust-Region Gradient Search with Numerical Derivatives

The starting point for the proposed algorithmic solution as well as the reference algorithm is the conventional trust-region (TR)-based gradient-search procedure (e.g., [20]). The algorithm produces a series $\boldsymbol{x}^{(i)}$, i = 0, 1, …, of approximations to the optimum design $\boldsymbol{x}^*$ by optimizing the linear model

$$\boldsymbol{L}^{(i)}(\boldsymbol{x}) = \boldsymbol{R}(\boldsymbol{x}^{(i)}) + \boldsymbol{J}_{\boldsymbol{R}}(\boldsymbol{x}^{(i)})\cdot(\boldsymbol{x}-\boldsymbol{x}^{(i)}) \tag{3}$$

of the response $\boldsymbol{R}$, established at the current iteration point $\boldsymbol{x}^{(i)}$. In (3), $\boldsymbol{J}_{\boldsymbol{R}}$ is the Jacobian matrix of $\boldsymbol{R}$, $\boldsymbol{J}_{\boldsymbol{R}} = [\boldsymbol{J}_1(\boldsymbol{x}) \ \ldots \ \boldsymbol{J}_n(\boldsymbol{x})] = [\partial\boldsymbol{R}/\partial x_1 \ \ldots \ \partial\boldsymbol{R}/\partial x_n]$, where $\boldsymbol{J}_k(\boldsymbol{x}) = \partial\boldsymbol{R}/\partial x_k$ represents a vector of all antenna response sensitivities w.r.t. the kth parameter. If available, $\boldsymbol{J}_{\boldsymbol{R}}$ can be evaluated using adjoint sensitivities [8] but, in vast majority of practical cases, it is estimated through finite differentiation, which incurs the cost of additional n EM analyses (n being dimensionality of the design space) per algorithm iteration. In the ith iteration of the TR algorithm, the following problem is solved

$$\boldsymbol{x}^{(i+1)} = \arg\min_{\boldsymbol{x};\ -\boldsymbol{d}^{(i)}\le\boldsymbol{x}-\boldsymbol{x}^{(i)}\le\boldsymbol{d}^{(i)}} U(\boldsymbol{L}^{(i)}(\boldsymbol{x})) \tag{4}$$

The vector $\boldsymbol{d}^{(i)}$ is the TR region size adjusted using the standard rules [22], i.e., based on the gain ratio $\rho = [U(\boldsymbol{R}(\boldsymbol{x}^{(i+1)})) - U(\boldsymbol{R}(\boldsymbol{x}^{(i)}))]/[U(\boldsymbol{L}^{(i)}(\boldsymbol{x}^{(i+1)})) - U(\boldsymbol{L}^{(i)}(\boldsymbol{x}^{(i)}))]$ (actual versus linear-model predicted objective function improvement). The inequalities $-\boldsymbol{d}^{(i)} \le \boldsymbol{x} - \boldsymbol{x}^{(i)} \le \boldsymbol{d}^{(i)}$ in (4) are understood component-wise. Because the variable ranges in antenna structures may be dramatically different for various parameters (e.g., fractions of millimetre for gaps, and tens of millimetres for ground plane width), the search region is defined here as a hypercube rather than a ball $\|\boldsymbol{x} - \boldsymbol{x}^{(i)}\| \le \delta^{(i)}$ (Euclidean norm with scalar TR radius). This—when setting up the initial size vector $\boldsymbol{d}^{(0)}$ proportional to the design space sizes—allows for ensuring similar treatment of variables with significantly different ranges.

2.3. Reduced-Cost Trust-Region Algorithm with Jacobian Update Management

The conventional TR algorithm with numerical derivatives updates the entire Jacobian after each successful iteration (i.e., when the candidate design found by (4) has been accepted due to a positive value of the gain ratio). As explained above, Jacobian updates essentially determine the computational cost of the optimization process. In the modified algorithm discussed here, the Jacobian matrix is updated only in part, depending, among others, on the relationship between the subsequent design vectors $\boldsymbol{x}^{(i+1)}$ and $\boldsymbol{x}^{(i)}$ and the TR region size $\boldsymbol{d}$, combined into $\varphi_k{}^i$ factors defined below

$$\varphi_k^i = \left| x_k^{(i+1)} - x_k^{(i)} \right| \Big/ d_k^{(i)}, \qquad k = 1, \ldots, n, \tag{5}$$

where $x_k{}^{(i)}$, $x_k{}^{(i+1)}$ and $d_k{}^{(i)}$ are the kth components of vectors $\boldsymbol{x}_k{}^{(i)}$, $\boldsymbol{x}_k{}^{(i+1)}$, and $\boldsymbol{d}^{(i)}$, respectively. The factors $\varphi_k{}^i$ relate the design change of the kth parameter with the TR region size $\boldsymbol{d}^{(i)}$ in the ith iteration. A decision about performing the update of the Jacobian $\boldsymbol{J_R}$ also depends on the optimization run history. The update history is examined in order to ensure that the part of the Jacobian $\boldsymbol{J_k}$, pertaining to the kth parameter, is computed at least once every few iterations. Other decision factors include user defined thresholds $0 < \varphi_{low} < \varphi_{high} < 1$, as well as the TR region size for the kth parameter $d_k{}^{(i)}$.

All the update decision factors are translated into a binary Jacobian update matrix $\boldsymbol{A^J}$ that stores the information about the future updates. The nonzero entries $\boldsymbol{a^J}_{k,i}$ refer to the Jacobian component $\boldsymbol{J}_k(\boldsymbol{x})$ that is to be updated in the next (or (i+1)th) iteration. If the update is omitted, the $\boldsymbol{J}_k$ value from the previous iteration is applied. The matrix $\boldsymbol{A^J}$ is created in the first iteration, and it is subsequently extended by adding an (i+1)th column upon each successful iteration.

The flow of the proposed reduced-cost TR region algorithm with sparse Jacobian updates is as follows:

1. Set the iteration index $i = 1$;
2. Initialize the Jacobian update matrix $\boldsymbol{A^J}$: $\boldsymbol{a^J}_{k,i} = 1$, $k = 1, \ldots, n$;
3. Update the Jacobian based on $\boldsymbol{A^J}$;
4. Find the candidate design $\boldsymbol{x}_{tmp}$ by solving (4);
5. Compute the gain ratio ρ and update the TR region size;
6. Perform a procedure of extending the $\boldsymbol{A^J}$ matrix:

if $\rho > 0$
  set $\boldsymbol{x}^{(i+1)} = \boldsymbol{x}_{tmp}$;
  for $k = 1, \ldots, n$, do
    set $\boldsymbol{a^J}_{k,i+1} = 1$, $F^k{}_{iter} = \sum_{j=\max(1,i-N_{iter}+1), \ldots, i} \boldsymbol{a^J}_{k,j}$;
    if $\{\|\boldsymbol{d}^{(i+1)}\| < \delta_{TR1}$ and $[(E == 0)$ or $(E == 1$ and $F^k{}_{iter} \geq 1)]\}$ or $\{\|\boldsymbol{d}^{(i+1)}\| \geq \delta_{TR1}$ and $\varphi_k{}^i < \varphi_{high}$ and $F^k{}_{iter} \geq 1\}$
      set $\boldsymbol{a^J}_{k,i+1} = 0$;
    end
  end
  set $i = i + 1$;
else
  if $\|\boldsymbol{d}^{(i+1)}\| < \delta_{TR1}$
    for $k = 1, \ldots, n$, do
      set $\boldsymbol{a^J}_{k,i} = 1$, $F^k{}_{iter} = \sum_{j=\max(1,i-N_{iter}+1), \ldots, i} \boldsymbol{a^J}_{k,j}$;
      if $\varphi_k{}^i < \varphi_{low}$ and $F^k{}_{iter} \geq 1$
        set $\boldsymbol{a^J}_{k,i} = 0$;
      end
    end
  elseif $(E == 1)$
    for $k = 1, \ldots, n$, do
      set $\boldsymbol{a^J}_{k,i} = 1$;
    end
  end
end

7. If the termination condition is not satisfied go to 3, else END.

In Step 2 of the algorithm, the matrix elements $\boldsymbol{a^J}_{k,i}$ are set to 1 for all $k = 1, \ldots, n$, so the entire Jacobian $\boldsymbol{J_R}(\boldsymbol{x}^{(0)})$ is computed through finite differentiation, for both basic and extended version of the algorithm. In the next iterations, the $\boldsymbol{J_R}$ update is performed depending on update matrix $\boldsymbol{A^J}$ (Step 3). In Step 4 the candidate design $\boldsymbol{x}_{tmp}$ if found by optimizing the objective function $U(\boldsymbol{L}(\boldsymbol{x}))$ using (4). In Step 5, the gain ratio ρ is computed and used to adjust the TR region size. The procedure of extending the decision matrix $\boldsymbol{A^J}$ (Step 6) is described in detail in the next paragraph.

In the paper, two versions of the reduced-cost TR region algorithm are introduced and compared, we will refer to these versions as a basic and extended one. The control parameter E is used to choose between the versions, $E = 0$ (basic) or $E = 1$ (extended). Both versions differ in terms of the update procedure of the matrix $\boldsymbol{A^J}$. The differences are highlighted in Table 1. In the basic version of the algorithm ($E = 0$), if the iteration is successful ($\rho > 0$), the update of the portion of Jacobian $\boldsymbol{J}_k$ is omitted in the two following cases, depending on the TR region size $\|\boldsymbol{d}^{(i+1)}\|$. If $\|\boldsymbol{d}^{(i+1)}\|$ is small, below a user-specified threshold δ_{TR1}, the update is not performed for all parameters $k = 1, \ldots, n$. Additionally, if the $\|\boldsymbol{d}^{(i+1)}\| > \delta_{TR1}$, the history of the updates is examined and, for each kth parameter, an indicator $F^k{}_{iter}$ is calculated as the number of performed updates in the last N_{iter} iterations. Subsequently, $\boldsymbol{J_k}$ is not computed if $F^k{}_{iter} \geq 1$ and if the $\varphi_k{}^i$ factor is below the user-specified threshold φ_{high}.

Table 1 The Comparison between the Basic and the Extended Version of the Proposed Algorithm

<table>
<tr><th rowspan="2">Algorithm version</th><th colspan="2">Step accepted ($\rho > 0$)
Add the (i+1)th column to the $\boldsymbol{A^J}$ matrix</th><th colspan="2">Step rejected ($\rho \leq 0$)
Alter the ith column of the $\boldsymbol{A^J}$ matrix</th></tr>
<tr><th>$\|\boldsymbol{d}^{(i+1)}\| < \delta_{TR1}$</th><th>$\|\boldsymbol{d}^{(i+1)}\| \geq \delta_{TR1}$</th><th>$\|\boldsymbol{d}^{(i+1)}\| < \delta_{TR1}$</th><th>$\|\boldsymbol{d}^{(i+1)}\| \geq \delta_{TR1}$</th></tr>
<tr><td>Basic ($E = 0$)</td><td>Skip update for all parameters</td><td rowspan="2">Check: update history for each parameter and if $\varphi_k{}^i < \varphi_{high}$</td><td rowspan="2">Check: update history for each parameter and if $\varphi_k{}^i < \varphi_{low}$</td><td>Do not alter the ith column of $\boldsymbol{A^J}$ matrix</td></tr>
<tr><td>Extended ($E = 1$)</td><td>Check update history for each parameter</td><td>Perform update for all parameters</td></tr>
</table>

For the extended version of the algorithm ($E = 1$), upon successful iteration, the Jacobian update is enforced for the small TR region size, $\|\boldsymbol{d}^{(i+1)}\| < \delta_{TR1}$, if the Jacobian was not updated in the last N_{iter} iterations, i.e., the checkup of the history of updates is in this case compulsory. If $\|\boldsymbol{d}^{(i+1)}\| > \delta_{TR1}$, both the history of the updates and the inequality $\varphi_k{}^i < \varphi_{high}$ are checked, just as it is done in the basic version.

If the candidate design is rejected ($\rho < 0$), the $\boldsymbol{A^J}$ matrix is extended in neither version of the algorithm. Moreover, in both versions, if $\|\boldsymbol{d}^{(i+1)}\| < \delta_{TR1}$, the respective portion of the Jacobian $\boldsymbol{J_k}$ is not calculated if both $\varphi_k{}^i < \varphi_{low}$ and $\boldsymbol{J_k}$ was updated at least once in the last N_{iter} iterations. The threshold value $\varphi_{low} < \varphi_{high}$ results in more frequent updates in order to make the linear model more accurate if the iterations are unsuccessful. If the step is rejected, in the case of large TR region size, $\|\boldsymbol{d}^{(i+1)}\| \geq \delta_{TR1}$, in the basic version, the old column of the $\boldsymbol{A^J}$ matrix is used and the update is performed accordingly. However, in the extended version, the update is enforced for all parameters, which ensures better accuracy of the linear model in the case of failed iteration.

The sparsity of Jacobian updates, introduced in the presented algorithm, allows for considerable reduction of the number of EM simulations during the optimization run as demonstrated in the next section. The savings are obtained at the expense of slight degradation of the design quality. The essence of the differences between the basic and the extended versions of the algorithm is highlighted below. The first difference is in handling the Jacobian updates when the algorithm is close to convergence, i.e., the condition $\|\boldsymbol{d}^{(i+1)}\| < \delta_{TR1}$ is satisfied. Here, the basic version unconditionally skips the finite-differentiation-based sensitivity updates and the rationale behind it is that potential changes of the Jacobian matrix at this point are minor and insignificant. The extended version takes into account the update history and carries out the update if it was not performed for the last few iterations. The second difference is in handling updates upon unsuccessful TR iterations: the basic version used the previously available Jacobian, whereas the extended version performs the update for all parameters thus making the Jacobian estimate more reliable. The implications of these differences as the following: (i) the extended algorithm performs the updates more often, therefore lower computational savings are expected as compared to the basic version; (ii) the extended version provides a slightly better estimation of the antenna sensitivities, therefore, improved quality of the design produced by the algorithm is expected. In other words, the two versions of the algorithm offer different trade-offs between the computational savings and the robustness. These expectations have been fully confirmed by the numerical results described in Section 3.

3. Verification Case Studies

This section provides the results of the numerical and experimental validation of the algorithm introduced in Section 2. Verification includes multiple optimization runs from random initial designs, statistical analysis to confirm the algorithm robustness, as well as comparison with the reference algorithm.

3.1. Benchmark Cases

The benchmark set consists of three UWB antennas shown in Fig. 1. Antenna I [23] is implemented on Taconic RF-35 substrate ($\varepsilon_r = 3.5$, $h = 0.762$ mm). The independent geometry parameters for this structure are $\boldsymbol{x} = [L_0\ dR\ R\ r_{rel}\ dL\ dw\ L_g\ L_1\ R_1\ dr\ c_{rel}]^T$. Antenna II [24] is implemented on FR4 substrate ($\varepsilon_r = 4.3$, $h = 1.55$ mm). The design parameters are $\boldsymbol{x} = [L_g\ L_0\ L_s\ W_s\ d\ dL\ d_s\ dW_s\ dW\ a\ b]^T$. Antenna III is based on the structure of [25] and implemented on RO4350 substrate ($\varepsilon_r = 3.48$, $h = 0.762$ mm); design variables are $\boldsymbol{x} = [L_0\ L_1\ L_2\ L\ dL\ L_g\ w_1\ w_2\ w\ dw\ L_s\ w_s\ c]^T$. The computational models for all structures are implemented in CST Microwave Studio and evaluated using its transient solver. The EM models incorporate SMA connectors.

3.2. Numerical Results

The benchmark antennas (cf. Section 3.1) have been optimized to attain minimum in-band reflection within the UWB frequency range of 3.1 GHz to 10.6 GHz. Detailed formulation of the optimization task has been discussed in Section 2.1. The algorithm of Section 2 has been executed with $\delta_{TR1} = 0.1$, $\varphi_{low} = 0.33$ and $\varphi_{high} = 0.66$, and several combinations of values of $N_{iter} = 3, 4, 5, 6$ and $E = 0, 1$. At the same time, the results are compared with those obtained using the reference algorithm (cf. Section 2.2). Furthermore, in order to carry out meaningful performance and robustness assessment, the optimization (for each combination of control parameters) has been executed 10 times with random initial designs. The statistical data has been gathered in Tables 2 and 3. Figures 2 through 4 show the initial and optimized reflection responses for a particular setup of the algorithm ($N_{iter} = 5$, $E = 1$). Figure 5 provides exemplary convergence plots for all considered antennas.

3.3. Discussion

The obtained results indicate that both versions of the proposed algorithm allow for considerable reduction of the optimization cost. The basic version provides us with savings from around 35 percent (for Antenna III) to around 50 percent (for Antenna I), with average savings being approximately 40 percent as compared to the reference algorithm.

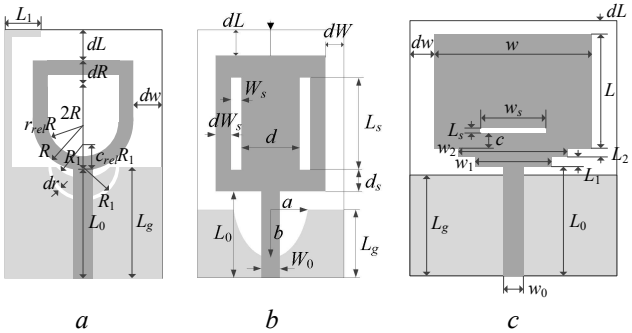

a *b* *c*

Fig. 1. *Antenna structures used for verification of the proposed algorithm. Ground plane marked using light gray shade.*
(a) *Antenna I [23],*
(b) *Antenna II [24],*
(c) *Antenna III [25].*

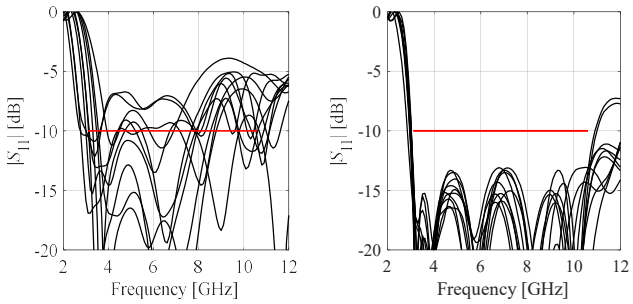

Fig. 2. *Reflection responses of Antenna I found using the proposed algorithm with N_{iter} = 5 and E = 1. Plots correspond to 10 random starting points. Horizontal line marks design specifications.*
***(a)** initial designs,*
***(b)** optimized designs.*

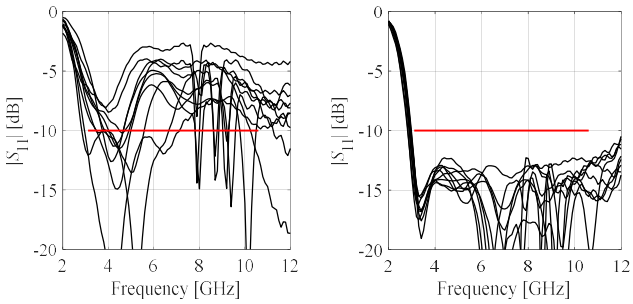

Fig. 3. *Reflection responses of Antenna II found using the proposed algorithm with N_{iter} = 5 and E = 1. Plots correspond to 10 random starting points. Horizontal line marks design specifications.*
***(a)** initial designs,*
***(b)** optimized designs.*

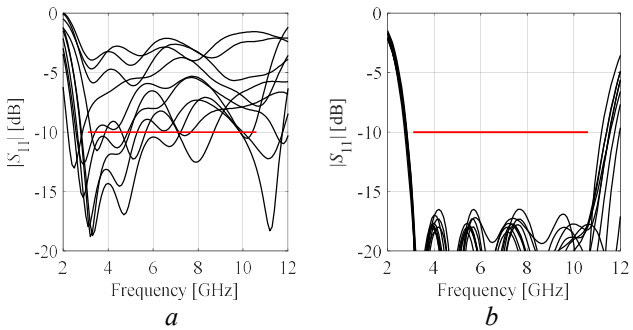

Fig. 4. *Reflection responses of Antenna I found using the proposed algorithm with N_{iter} = 5 and E = 1. Plots correspond to 10 random starting points. Horizontal line marks design specifications.*
***(a)** initial designs,*
***(b)** optimized designs.*

For the extended version, the reduction of the number of EM simulations is lower (from around 25 percent for Antenna III to over 35 percent for Antenna I). On the other hand, degradation of the design quality is practically acceptable for both algorithms (around 1.2 dB on average, cf. Table 3), yet better solution quality is obtained for the extended version (around 0.7 dB on average), as expected.

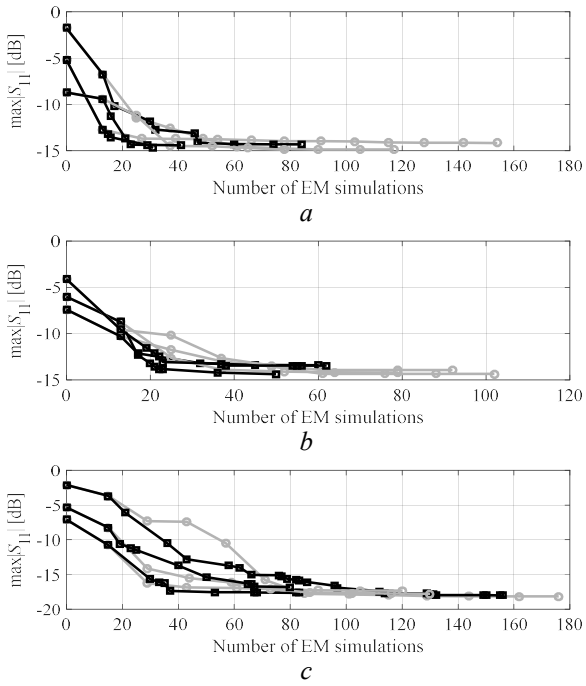

Fig. 5. *Convergence plots for selected algorithm runs: reference algorithm (gray) and the proposed algorithm with N_{iter} = 5 and E = 1 (black).*
***(a)** Antenna I,*
***(b)** Antenna II,*
***(c)** Antenna III.*

Table 2 Optimization Results for Antennas I through III: Algorithm Cost and Objective Function Values

Algorithm		Antenna I Cost*	Antenna I Max $\|S_{11}\|$#	Antenna II Cost*	Antenna II Max $\|S_{11}\|$#	Antenna III Cost*	Antenna III max $\|S_{11}\|$#
Reference TR algorithm		111.2	−14.8	111	−13.7	139.7	−17.5
Basic	N_{iter} = 3	58.3	−13.7	73.1	−12.7	91.2	−16.3
	N_{iter} = 4	52.6	−13.6	71.0	−12.5	88.8	−16.4
	N_{iter} = 5	56.4	−13.6	72.7	−12.8	87.5	−15.8
	N_{iter} = 6	51.7	−13.6	62.0	−12.5	87.0	−15.8
Extended	N_{iter} = 3	73.0	−14.2	87.4	−12.9	101.5	−16.8
	N_{iter} = 4	69.8	−14.2	80.6	−12.9	104.4	−16.9
	N_{iter} = 5	70.3	−14.2	74.7	−12.9	100.3	−16.9
	N_{iter} = 6	70.2	−14.2	79.3	−12.9	102.4	−16.9

* Number of EM simulations averaged over 10 algorithm runs (random initial points).
# Maximum $|S_{11}|$ within UWB frequency range (averaged over 10 algorithm runs).

It should be mentioned that in many cases, especially for variable-fidelity optimization procedures [1], [10], reduction of the design cost is of primary importance (e.g., when solving sub-problems at lower fidelity of EM models), whereas solution accuracy comes secondary due to iterative correction procedures utilized in these algorithms. The study of the effect of the parameter N_{iter} indicates that, in general, larger values are preferred in terms of ensuring better computational savings, however, certain fluctuations can be observed for some antennas, partially resulting from the statistical nature of the results gathered in the tables.

The convergence plots shown in Fig. 5 indicate that the proposed algorithm exhibits consistent behavior across the considered benchmark antennas, in particular, leads to a faster termination of the optimization algorithm without compromising design quality (as already indicated in Tables 2 and 3). In many cases, it also leads to a faster reduction of the objective function value as compared with the reference algorithm.

3.4. Experimental Validation

Selected designs of Antennas I, II, and III have been fabricated and tested to validate the computational models utilized in the optimization process. Figure 6 shows the fabricated antenna prototypes, whereas Figs. 7 through 9 show the simulated and measured reflection responses, realized gain characteristics, as well as H- and E-plane radiation patterns at 4 GHz, 6 GHz and 8 GHz. The agreement between simulations and measurements is good. Some discrepancies, particularly for the E-plane patterns, are mostly the results of the measurement setup (90-degree bend used to mount the antennas).

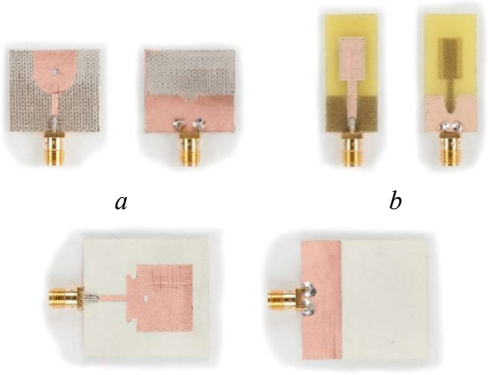

a *b* *c*

Fig. 6. *Photographs of fabricated antenna prototypes, front (left) and back (right).*
(a) *Antenna I,*
(b) *Antenna II,*
(c) *Antenna III.*

Table 3 Optimization Results for Antennas I through III: Computational Savings and Design Quality

Algorithm		Antenna I		Antenna II		Antenna III	
		Cost savings* [%]	Δ max $\|S_{11}\|$# [dB]	Cost savings* [%]	Δ max $\|S_{11}\|$# [dB]	Cost savings* [%]	Δ max $\|S_{11}\|$# [dB]
Basic	$N_{iter} = 3$	47.6	1.1	34.1	1.0	34.7	1.2
	$N_{iter} = 4$	52.7	1.2	36.0	1.2	36.4	1.1
	$N_{iter} = 5$	49.3	1.2	34.5	0.9	37.4	1.7
	$N_{iter} = 6$	53.5	1.2	44.4	1.2	37.7	1.7
Extended	$N_{iter} = 3$	34.4	0.6	21.3	0.9	27.3	0.7
	$N_{iter} = 4$	37.2	0.6	27.4	0.9	25.3	0.6
	$N_{iter} = 5$	36.8	0.6	32.7	0.9	28.2	0.6
	$N_{iter} = 6$	36.9	0.6	28.6	0.9	26.7	0.6

* Percentage-wise cost savings w.r.t. the reference algorithm.
# Degradation of objective function value w.r.t. the reference algorithm.

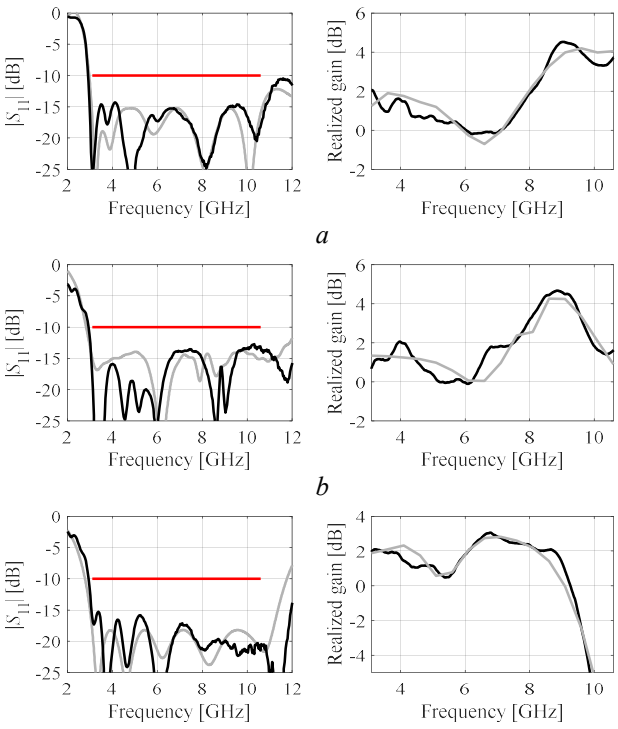

Fig. 7. *Simulated (gray) and measured (black) reflection responses and realized gain characteristics of the fabricated antenna prototypes.*
(a) *Antenna I,*
(b) *Antenna II,*
(c) *Antenna III.*

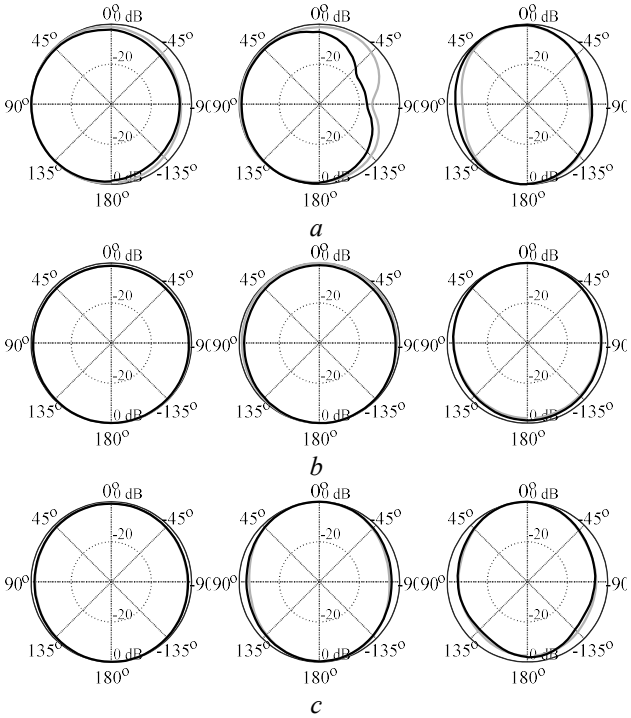

Fig. 8. *Simulated (gray) and measured (black) H-plane radiation patterns of the fabricated antenna prototypes at 4 GHz (left), 6 GHz (middle), and 8 GHz (right).*
(a) *Antenna I,*
(b) *Antenna II,*
(c) *Antenna III.*

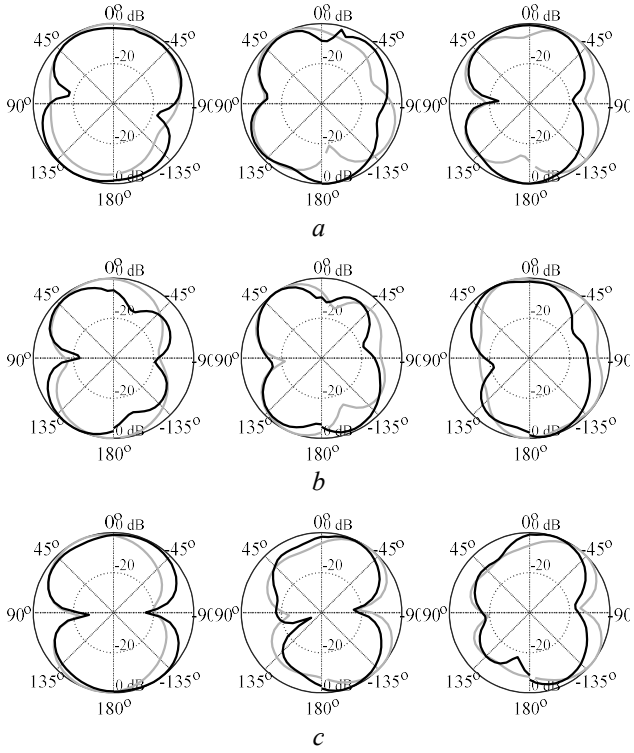

Fig. 9. *Simulated (gray) and measured (black) E-plane radiation patterns of the fabricated antenna prototypes at 4 GHz (left), 6 GHz (middle), and 8 GHz (right).*
(a) *Antenna I,*
(b) *Antenna II,*
(c) *Antenna III.*

4. Conclusion

In this work, a reduced-cost trust-region-embedded gradient search algorithm for design optimization of antenna structures has been presented. The foundation of the algorithm is sparse updating of the antenna response Jacobian matrix with the updates controlled by relative relocation of the design variable vectors between algorithm iterations, optimization history, as well as the search region size. Combination of these factors permits considerable reduction of the optimization cost (in terms of the number of EM simulations of the antenna at hand). At the same time, the final design quality is only slightly degraded as compared to the reference algorithm. The speed/quality trade-offs can be adjusted using the algorithm control parameters.

The proposed procedure has been extensively validated using a set of benchmark wideband antenna structures. The average computational savings are as high as 40 percent (w.r.t. to the conventional TR algorithm). The proposed algorithm can be applied to direct optimization of high-fidelity EM simulation models of antennas but also to accelerate solving of optimization sub-problems in surrogate-assisted design procedures, especially those exploiting variable-fidelity EM models. These applications will be the subject of the future work.

5. Acknowledgments

The authors thank Dassault Systemes, France, for making CST Microwave Studio available. This work is partially supported by the Icelandic Centre for Research (RANNIS) Grant 174114051, and by National Science Centre of Poland Grant 2015/17/B/ST6/01857.

6. References

[1] S. Koziel and S. Ogurtsov, *Antenna design by simulation-driven optimization. Surrogate-based approach*. Springer, New York, 2014.

[2] J. Nocedal, S.J. Wright, *Numerical Optimization*, 2nd edition, Springer, New York, 2006.

[3] T.G. Kolda, R.M. Lewis, and V. Torczon, "Optimization by direct search: new perspectives on some classical and modern methods," SIAM Review, vol. 45, no. 3, pp. 385–482, 2003.

[4] S. Soltani, P. Lotfi, and R.D. Murch, "Design and optimization of multiport pixel antennas," *IEEE Trans. Ant. Prop.*, vol. 66, no. 4, pp. 2049-2054, 2018.

[5] S. K. Goudos, K. Siakavara, T. Samaras, E. E. Vafiadis, and J. N. Sahalos, "Self-adaptive differential evolution applied to real-valued antenna and microwave design problems," *IEEE Trans. Antennas Propag.*, vol. 59, no. 4, pp. 1286–1298, Apr. 2011.

[6] A. Lalbakhsh, M.U. Afzal, K.P. Esselle, "Multiobjective particle swarm optimization to design a time-delay equalizer metasurface for an electromagnetic band-gap resonator antenna," *IEEE Ant. Wireless Prop. Lett.*, vol. 16, pp. 912-915, 2017.

[7] M. Ghassemi, M. Bakr, and N. Sangary, "Antenna design exploiting adjoint sensitivity-based geometry evolution," *IET Microwaves Ant. Prop.*, vol. 7, no. 4, pp. 268-276, 2013.

[8] S. Koziel, F. Mosler, S. Reitzinger, and P. Thoma, "Robust microwave design optimization using adjoint sensitivity and trust regions," *Int. J. RF and Microwave CAE*, vol. 22, no. 1, pp. 10-19, 2012.

[9] CST Microwave Studio, ver. 2015, CST AG, Bad Nauheimer Str. 19, D-64289 Darmstadt, Germany, 2015.

[10] S. Koziel and A. Bekasiewicz. *Multi-objective design of antennas using surrogate models*. World Scientific, 2016.

[11] J. Zhu, J.W. Bandler, N.K. Nikolova and S. Koziel, "Antenna optimization through space mapping," *IEEE Transactions on Antennas and Propagation*, vol. 55, no. 3, pp. 651-658, March 2007.

[12] S. Koziel and S. Ogurtsov, "Design optimization of antennas using electromagnetic simulations and adaptive response correction technique," *IET Microwaves, Antennas Prop.*, vol. 8, no. 3, pp. 180-185, 2014.

[13] S. Koziel and L. Leifsson, "Simulation-driven design by knowledge-based response correction techniques," Springer, 2016.

[14] S. Koziel, "Fast simulation-driven antenna design using response-feature surrogates," *Int. J. RF & Microwave CAE*, vol. 25, no. 5, pp. 394-402, 2015.

[15] S. Koziel and S.D. Unnsteinsson, "Accelerated design optimization of antenna structures using adaptive response scaling," *IEEE Int. Symp. Ant. Prop.*, 2018.

[16] B. Liu, S. Koziel, and Q. Zhang, "A multi-fidelity surrogate-model-assisted evolutionary algorithm for computationally expensive optimization problems," *J. Comp. Sc.*, vol. 12, pp. 28-37, 2016.

[17] D.I.L. de Villiers, I. Couckuyt, and T. Dhaene, "Multi-objective optimization of reflector antennas using kriging and probability of improvement," *Int. Symp. Ant. Prop.*, pp. 985-986, San Diego, USA, 2017.

[18] J.P. Jacobs, "Characterization by Gaussian processes of finite substrate size effects on gain patterns of microstrip antennas,"

IET Microwaves Ant. Prop., vol. 10, no. 11, pp. 1189-1195, 2016.

[19] S. Koziel, and A. Bekasiewicz "Statistical analysis and robust design of circularly polarized antennas using sequential approximate optimization," *IEEE Int. Microwave and Radar Conference (MIKON)*, 2018.

[20] S. Koziel, Q.S. Cheng, and S. Li, "Optimization-driven antenna design framework with multiple performance constraints," *Int. J. RF Microwave CAE*, vol. 28, no. 4, 2018.

[21] Y.H. Chiu, and Y.S. Chen, "Multi-objective optimization of UWB antennas in impedance matching, gain, and fidelity factor," *IEEE Int. Symp. Ant. Prop.*, pp. 1940-1941, 2015.

[22] A.R. Conn, N.I.M. Gould, and P.L. Toint, *Trust Region Methods*, MPS-SIAM Series on Optimization, 2000.

[23] M.G.N. Alsath and M. Kanagasabai, "Compact UWB monopole antenna for automotive communications, *IEEE Trans. Ant. Prop.*, vol. 63, no. 9, pp. 4204-4208, 2015.

[24] M.A. Haq, S. Koziel, and Q.S. Cheng, "EM-driven size reduction of UWB antennas with ground plane modifications," *Int. Applied Comp. Electromagnetics Society (ACES China) Symposium*, 2017.

[25] D.R. Suryawanshi and B.A. Singh, "A compact UWB rectangular slotted monopole antenna," *IEEE Int. Conf. Control, Instrumentation, Comm. Comp. Tech. (ICCICCT)*, pp. 1130-1136, 2014.